Inorg. Chem. **2006**, *45*, 3976–3982

2D Hydrogen-Bonded Square-Grid Coordination Networks with a Substitution-Active Metal Site

Kanji Takaoka,[†,‡] Masaki Kawano,*[,†,‡] Toshiya Hozumi,[†] Shin-ichi Ohkoshi,[†] and Makoto Fujita*[,†,‡]

Department of Applied Chemistry, School of Engineering, The University of Tokyo, 7-3-1 Hongo, Bunkyo-ku, Tokyo 113-8656, Japan, and Genesis Research Institute, Inc., 4-1-35 Noritake-Shinmachi, Nishi-ku, Nagoya, Aichi 451-0051, Japan

Received December 14, 2005

Reported here is the preparation and property of 2D coordination networks composed of rodlike ligands with ethylene glycol side chains (**1**). Two 2D coordination networks, $\{[Co(\mathbf{1})_2(H_2O)_2](NO_3)_2 \cdot 1.5H_2O\}_n$ and $\{[Ni(\mathbf{1})_2(H_2O)_2](NO_3)_2 \cdot 1.5H_2O\}_n$, have been synthesized and characterized by single-crystal X-ray diffraction, TG, DSC, UV–vis spectroscopy, and magnetic measurements. The structural analyses clarified that infinite 1D hydrogen-bond arrays composed of ethylene glycol chains contribute to the stabilization of 2D coordination frameworks, keeping the environment of substitution-active metal sites unchanged. They are more stable than a similar square-grid coordination network that does not possess an ethylene glycol chain on the ligand. We also succeeded in the direct observation of a reversible apical-ligand-exchange reaction at the cobalt(II) and nickel(II) ions in a single-crystal-to-single-crystal fashion because of the considerable stability as well as moderate flexibility of the framework. The cobalt-containing coordination network crystal showed chromic behavior depending on temperatures. Crystallographic and spectroscopic studies revealed that the color change of the crystal was attributed to the ligand-exchange process between H_2O and a NO_3 anion on the cobalt metal. Magnetic measurements indicated weak antiferromagnetic nearest-neighbor spin coupling between cobalt(II) ions.

Introduction

Porous coordination networks have been widely prepared via self-assembly of metal ions with designed molecular building blocks. They have attracted considerable attention because of their unique physical properties.[1] In sharp contrast to robust inorganic materials such as zeolite, one of the salient features of coordination networks is that they can be remarkably flexible and be crystallized. The flexibility is an intriguing feature for developing a new functional property as porous dynamic materials. The capability to prepare a single crystal also has several advantages in that one can definitively determine a crystal structure including guest molecules and design new functional materials on the basis of structural knowledge at the atomic level. However, to develop a new class of materials using a coordination framework, it is essential to improve the stability while keeping the material's unique properties. In the case of coordination networks composed of 2D layers, the interactions between 2D layers prompted us to study the stability of the structure during guest removal/re-inclusion processes. For example, the intercalation of pillared-layer motifs between layers using a coordination bond is a simple and rational method for designing more-rigid frameworks.[2,3] Otherwise, the connection of 2D layers via a hydrogen bond[4] is also useful for the construction of robust coordination frameworks while maintaining the function of the transition-

* To whom correspondence should be addressed. E-mail: mkawano@appchem.t.u-tokyo.ac.jp (M.K.); mfujita@appchem.t.u-tokyo.ac.jp (M.F.).
† The University of Tokyo.
‡ Genesis Research Institute, Inc.

(1) (a) Batten, S. R.; Robson, R. *Angew. Chem., Int. Ed.* **1998**, *37*, 1460. (b) Moulton, B.; Zaworotko, M. J. *Chem. Rev.* **2001**, *101*, 1629. (c) Eddaoudi, M.; Moler, D. B.; Li, H.; Chen, B.; Reineke, T. M.; O'Keeffe, M.; Yaghi, O. M. *Acc. Chem. Res.* **2001**, *34*, 319. (d) Yaghi, O. M.; O'Keeffe, M.; Ockwig, N. W.; Chae, H. K.; Eddaoudi, M.; Kim, J. *Nature* **2003**, *423*, 705. (e) Kitagawa, S.; Kitaura, R.; Noro, S. *Angew. Chem., Int. Ed.* **2004**, *43*, 2334. (f) Janiak, C. *Dalton Trans.* **2003**, 2781. (g) James, S. L. *Chem. Soc. Rev.* **2003**, *32*, 276. (h) Braga, D. *Chem. Commun.* **2003**, 2751.

(2) (a) Kondo, M.; Okubo, T.; Asami, A.; Noro, S.-I.; Yoshitomi, T.; Kitagawa, S.; Ishii, T.; Matsuzaka, H.; Seki, K. *Angew. Chem., Int. Ed.* **1999**, *38*, 140. (b) Alberti, G.; Brunet, E.; Dionigi, C.; Juanes, O.; Mata, M. J. D.; RodrIguez-Ubis, J. C.; Vivani, R. *Angew. Chem., Int. Ed.* **1999**, *38*, 3351. (c) Kitaura, R.; Fujimoto, K.; Noro, S.; Kondo, M,; Kitagawa, S. *Angew. Chem., Int. Ed*. **2002**, *41*, 133. (d) Hung, L.; Wang, S. L.; Kao, H. M.; Lii, K. H. *Inorg. Chem*. **2002**, *41*, 3929. (e) Chang, W. K.; Chiang, R. K.; Jiang, Y. C.; Wang. S. L.; Lee, S. F.; Lii, K. H. *Inorg. Chem*. **2004**, *43*, 2564. (f) Chun, H.; Dyunuk, D.; Kim, K. *Chem.—Eur. J.* **2005**, *11*, 3521.

10.1021/ic052138u CCC: $33.50
Published on Web 04/21/2006

metal ions, because coordination sites are not used in binding layers. At the same time, a hydrogen bond will reinforce the structural flexibility of coordination networks via reversible bond formation against structural distortion.

In this study, we focused on the design of a more-rigid as well as flexible coordination framework by utilizing a hydrogen bond. The formation of square-grid coordination networks with rodlike ligands is predictable because of simplicity, making it possible to synthesize novel networks with a highly controlled framework and cavity. During the past decade, we have studied the preparation of square-grid complexes with guest-inclusion and -exchange properties.[5] The strategy for introducing a hydrogen bond is the modification of a bridging ligand while keeping the main framework. Herein, we report the preparation and properties of 2D coordination networks that involve rodlike ligands with ethylene glycol side chains (**1**). We have found that they are more stable than a similar square-grid coordination network that does not possess an ethylene glycol chain on the ligand. Moreover, we also report that substitution-active metal sites are incorporated in the square grid coordination networks. One of original features of coordination networks is that it often contains substitution-active metal sites in the framework. Ligand exchange will considerably affect d-orbital configuration, leading to electronic and spin control of coordination networks. Crystallographic studies of a number of coordination polymers were reported;[6] however, there are a few reports on a ligand-exchange process observed by single-crystal X-ray diffraction analysis, because the drastic structural change during the process readily causes the loss of crystallinity.[7,8] Recently, we communicated a preliminary result on the in situ observation of a reversible single-crystal-to-single-crystal transformation of apical-ligand exchange on cobalt metals accompanied by the removal/inclusion process of water molecules.[7] The details will be discussed here as well.

Results and Discussion

Synthetic Strategy. The combination of a linear rodlike ligand and transition metals is suitable for preparation of a 2D layer square-grid network. One can readily modify the environment of a cavity in the 2D network by introducing functional groups into the bridging phenylene ring. We designed a 4-pyridyl-terminated rodlike ligand with ethylene glycol side chains (**1**), as shown in eq 1.

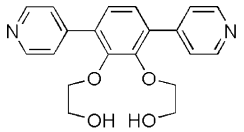

1

$$+\ Co(NO_3)_2\cdot 6H_2O \longrightarrow \{[Co(II)(\mathbf{1})_2(H_2O)_2](NO_3)_2\cdot 1.5H_2O\}_n \qquad (1)$$

2

The ethylene glycol chain can be expected to play the following roles: first, it will contribute to hydrogen-bond formation. Each 2D layer can be connected via hydrogen bonding without changing the framework. Second, the flexibility of the ethylene glycol chain will provide the cavity with a solution-like fluid environment in the solid state.

Structure. The layering diffusion of a methanol solution of $Co(NO_3)_2\cdot 6H_2O$ into a toluene/methanol solution of **1** at room temperature for 4 days resulted in the single-crystal formation of complex $\{[Co(\mathbf{1})_2(H_2O)_2](NO_3)_2\cdot 1.5H_2O\}_n$ (**2**) in 76% yield (eq 1). X-ray crystallographic analysis revealed the formation of a noninterpenetrated 15.7 × 15.7 Å^2 square-grid coordination polymer (Figure 1a). The cobalt(II) center is octahedrally coordinated to four pyridyl groups of **1** at the equatorial positions ($Co-N_{Py_1}$, 2.160(3) Å; $Co-N_{Py_2}$, 2.142(3) Å) and two water molecules at the apical positions ($Co-O_{H_2O}$, 2.095(4) Å).[9] Disordered water molecules and

(3) The charge-assisted hydrogen bonds also used by Ward et al. in crystal engineering studies: (a) Russell, V. A.; Evans, C. C.; Li, W. J.; Ward, M. D. *Science* **1997**, *276*, 575. (b) Evans, C. C.; Sukarto, L.; Ward, M. D. *J. Am. Chem. Soc.* **1999**, *121*, 320. (c) Holman, K. T.; Ward, M. D. *Angew. Chem., Int. Ed.* **2000**, *39*, 1653. (d) Holman, K. T.; Pivovar, A. D.; Ward, M. D. *Science* **2001**, *294*, 1907.

(4) (a) Cheng, D.; Khan, M. A.; Houser, R. P. *Inorg. Chem.* **2001**, *40*, 6858. (b) Uemura, K.; Kitagawa, S.; Kondo, M.; Fukui, K.; Kitaura, R.; Cheng, H.-C.; Mizutani, T. *Chem.—Eur. J.* **2002**, *8*, 3586. (c) Uemura, K.; Kitagawa, S.; Fukui, K.; Saito, K. *J. Am. Chem. Soc.* **2004**, *126*, 3817. (d) Liu, Y.-H.; Wu, H.-C. Lin, H.-M.; Hou, W.-H.; Lu, K.-L. *Chem. Commun.* **2003**, 60. (e) Kumar, D. K.; Jose, D. A.; Das, A.; Dastidar, P. *Inorg. Chem.* **2005**, *44*, 6933.

(5) (a) Fujita, M.; Kwon, Y. J.; Washizu, S.; Ogura, K. *J. Am. Chem. Soc.* **1994**, *116*, 1151. (b) Biradha, K.; Fujita, M. *J. Chem. Soc., Dalton Trans.* **2000**, 3805. (c) Biradha, K.; Hongo, Y.; Fujita, M. *Angew. Chem., Int. Ed.* **2000**, *39*, 3805. (d) Biradha, K.; Hongo, Y.; Fujita, M. *Angew. Chem., Int. Ed.* **2002**, *31*, 3395. (e) Ohmori, O.; Kawano, M.; Fujita, M. *CrystEngComm* **2004**, *6*, 51.

(6) For single-crystal-to-single-crystal transformation in coordination networks, see: (a) Li, H.; Eddaoudi, M.; O'Keeffe, M.; Yaghi, O. M. *Nature* **1999**, *402*, 276. (b) Chui, S. S.-Y.; Lo, S. M.-F.; Charmant, J. P. H.; Orpen, A. G.; Williams, I. D. *Science* **1999**, *283*, 1148. (c) Kepert, C. J.; Rosseinsky, M. J. *Chem. Commun.* **1999**, 375. (d) Biradha, K.; Fujita, M. *Angew. Chem., Int. Ed.* **2002**, *41*, 3392. (e) Ohmori, O.; Kawano, M.; Fujita, M. *J. Am. Chem. Soc.* **2004**, *126*, 16292. (f) Ohmori, O.; Kawano, M.; Fujita, M. *Angew. Chem., Int. Ed.* **2005**, *44*, 1962. (g) Suh, M. P.; Ko, W. J.; Choi, H. J. *J. Am. Chem. Soc.* **2002**, *124*, 10976. (h) Lee, E. Y.; Suh, M. P. *Angew. Chem., Int. Ed.* **2004**, *43*, 2798. (i) Choi, H. J.; Suh, M. P. *J. Am. Chem. Soc.* **2004**, *126*, 15844. (j) Takamizawa, S.; Nakata, E.; Yokoyama, H.; Mochizuki, K.; Mori, W. *Angew. Chem., Int. Ed.* **2003**, *42*, 4331. (k) Takamizawa, S.; Nakata, E.; Saito, T. *Angew. Chem., Int. Ed.* **2004**, *43*, 1368. (l) Abrahams, B. F.; Moylan, M.; Orchard, S. D.; Robson, R. *Angew. Chem., Int. Ed.* **2003**, *42*, 1848. (m) Maji, T. K.; Uemura, K.; Chang, H.-C.; Matsuda, R.; Kitagawa, S. *Angew. Chem., Int. Ed.* **2004**, *43*, 3269. (n) Rather, B.; Zaworotko, M. J. *Chem. Commun.* **2003**, 830. (o) Halder, G. J.; Kepert, C. J.; Moubaraki, B.; Murray, K. S.; Cashion, J. D. *Science* **2002**, *298*, 1762. (p) Su, C.-Y.; Goforth, A. M.; Smith, M. D.; Pellechia, P. J.; zur Loye, H. C. *J. Am. Chem. Soc.* **2004**, *126*, 3576. (q) Dybtsev, D. N.; Chun, H.; Kim, K. *Angew. Chem., Int. Ed.* **2004**, *43*, 5033. (r) Zeng, M.-H.; Feng, X.-L.; Chen, X.-M. *Dalton Trans.* **2004**, 2217. (s) Wu, C.-D.; Lin, W. *Angew. Chem., Int. Ed.* **2005**, *44*, 1958. (t) Michaelides, A.; Skoulika, S. *Cryst. Growth Des.* **2005**, *5*, 529. (u) Deliters, E.; Bulach, V.; Hosseini, M. *Chem. Commun.* **2005**, 3906. (v) Ma, J.-P.; Dong, Y.-B.; Huang, R.-Q.; Smith, M. D.; Su, C.-Y. *Inorg. Chem.* **2005**, *44*, 6143. (w) Toh, N. L.; Nagarathinam, M.; Vittal, J. J. *Angew. Chem., Int. Ed.* **2005**, *44*, 2237. (x) Chu, Q.; Swenson, D. C.; MacGillivray, L. R. *Angew. Chem., Int. Ed.* **2005**, *44*, 3569.

(7) Takaoka, K.; Kawano, M.; Tominaga, M.; Fujita, M. *Angew. Chem., Int. Ed.* **2005**, *44*, 2151.

(8) (a) Hanson, K.; Calin, N.; Bugaris, D.; Scancela, M.; Sevov, S. C. *J. Am. Chem. Soc.* **2004**, *126*, 10502. (b) Chen, C.-L.; Goforth, A. M.; Smith, M. D.; Su, C.-Y.; zur Loye, H. C. *Angew. Chem., Int. Ed.* **2005**, *44*, 6673. (c) Hu, C.; Englert, U. *Angew. Chem., Int. Ed.* **2005**, *44*, 2281. (d) Zhang, J.-P.; Lin, Y.-Y.; Zhang, W.-X.; Chen, X.-M. *J. Am. Chem. Soc.* **2005**, *127*, 14162.

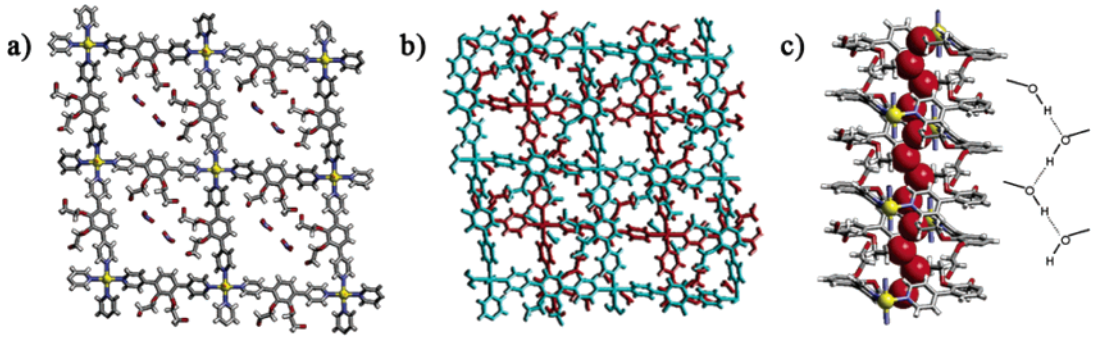

Figure 1. (a) Square-grid network of $\{[Co(\mathbf{1})_2(H_2O)_2](NO_3)_2 \cdot 1.5H_2O\}_n$ (**2**). Guest molecules (H_2O) are omitted for clarity. (b) Two-layer stack of **2**. (c) Infinite 1D hydrogen-bond (O−H···O) array in **2**. Oxygen atoms of OH groups are represented by the space-filling model.

two nitrate anions occupy the square cavities. The distances between the cobalt ion and the nearest oxygen atom of nitrate anions are in the range of 4.2−4.4 Å. The grid sheet layers are stacked on each other in an offset fashion on both edges (Figure 1b). A remarkable feature of the X-ray crystal structure is that there are infinite 1D hydrogen-bond (O−H···O) arrays composed of OH groups of the ligand through the cavity channel. In the 1D hydrogen-bond array, the hydrogen-bond length between ethylene glycol chains (O···O distance is ca. 2.60 Å) is particularly short despite the absence of charged species (Figure 1c).[10] On the other hand, the neighboring layers have an interlayer separation of 4.2 Å, where there is no $\pi-\pi$ interactions between the layers.

To investigate the effect of ethylene glycol side chains, we synthesized a square framework composed of the ligand with no substituent. The reaction of compound **4** with $Co(NO_3)_2 \cdot 6H_2O$ in a 2:1 ratio in methanol resulted in the same square-grid coordination polymer $\{[Co(\mathbf{4})_2(H_2O)_2](NO_3)_2 \cdot 2H_2O \cdot 2CH_3OH\}_n$ (**5**) (eq 2).

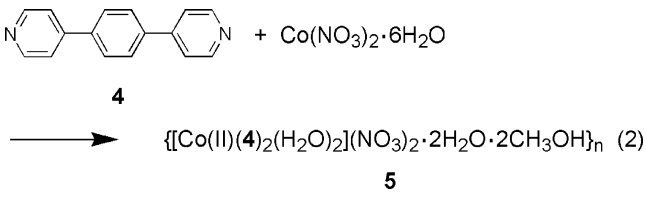

As expected, the crystal packing of **5** is similar to that of **2** (Figure 2). The distance (3.7 Å) between the planes of the phenyl ring of the neighboring layers is shorter than that in **2**.

Thermal Stability of 2 and 5. Thermogravimetric analysis on the crystal of **2** showed loss of all water molecules in the range of 25−90 °C (see the Supporting Information, Figure S1). The amount of dehydrated water molecules (6.47%) was in excellent agreement with that of water molecules determined by X-ray analysis (calcd: 6.6%). DSC analysis on the crystal of **2** showed two endothermic peaks at 93.8 and

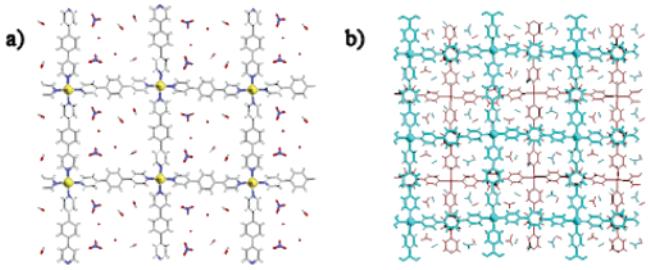

Figure 2. (a) Square-grid network of $\{[Co(\mathbf{4})_2(H_2O)_2](NO_3)_2 \cdot 2H_2O \cdot 2CH_3OH\}_n$ (**5**). (b) Two-layer stack of **5**.

77.4 °C during the dehydration process, which may be attributed to two kinds of water molecules; that is, the one coordinating to a Co atom and the other present as a guest molecule. However, **5** showed a gradual deterioration of crystallinity from room temperature, followed by no diffraction at 60 °C. In addition, thermogravimetric analysis of **5** showed that the chemical decomposition temperature of **5** (170 °C) was considerably lower than that of **2** (220 °C) (see the Supporting Information, Figure S2). These results indicate that the ethylene glycol chains significantly contribute to the stability of **2** and that the introduction of proper functional groups can improve the stability of a coordination framework.

Direct Observation of Substitution-Active Metal Sites of 2 and 3. The single crystallinity of **2** was not lost even after removal of all water molecules by heating the crystal at 423 K for 24 h. Moreover, the dehydration process caused a clear color change from yellow to red. The structure determination of the dehydrated crystal $[Co(\mathbf{1})_2(NO_3)_2]_n$ (**6**) shows that the crystal system and space group remain the same as those of **2**. The X-ray structure of **6** elucidated that two nitrate anions are coordinated to the apical position of a Co atom (nitrate form, Figure 3b) instead of water molecules (aqua form, Figure 3a). The coordinated nitrate anions caused the 2D layers to change electrically from cationic to neutral. The X-ray analysis revealed that there was no sliding of 2D layers. It may be mainly attributable to infinite 1D hydrogen-bond arrays that play a crucial role in the binding forces between the layers. New hydrogen-bond formation between OH groups of **1** and nitrate ions coordinated to Co atoms also has a stabilizing effect on the framework.

(9) These values are typical of Co(II)−pyridyl aqua complexes: (a) Felloni, M.; Blake, A. J.; Champness, N. R.; Hubberstey, P.; Wilson, C.; Schröder, M. *J. Supramol. Chem.* **2002**, 163. (b) Banfi, S.; Carlucci, L.; Caruso, E.; Ciani, G.; Proserpio, D. *J. Chem. Soc., Dalton Trans.* **2002**, 2714.

(10) Hong, B. G.; Lee, J. Y.; Lee, C.-W.; Kim, J. C.; Bae, S. C.; Kim, K. S. *J. Am. Chem. Soc.* **2001**, *123*, 10748.

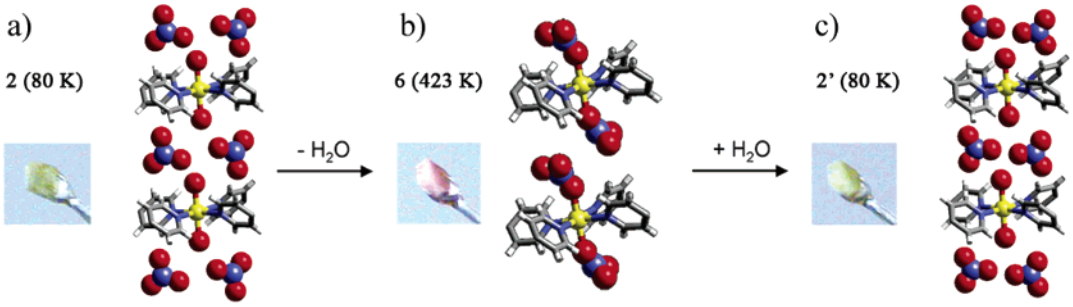

Figure 3. Photographs of crystals and structures around the cobalt ion of (a) the original crystal **2**, (b) the crystal after heating at 423 K for 24 h (**6**), and (c) the crystal after exposure of **6** to air (**2′**). Two other disordered nitrate anions are omitted for clarity.

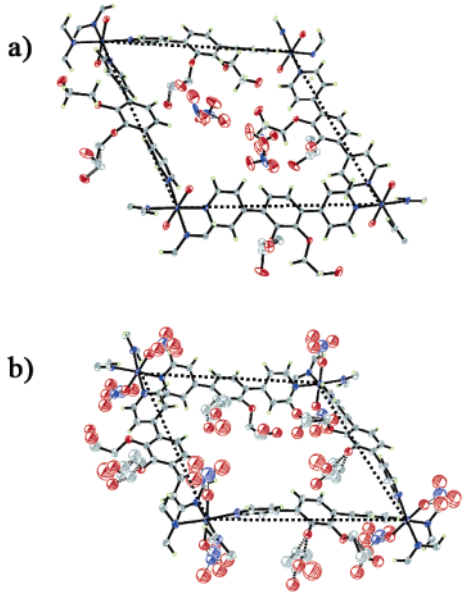

Figure 4. ORTEP drawing (30% probability level) of a square-grid unit of (a) **2** and (b) **6**. The bridging ligand of **6** shows considerable distortion compared to that of **2**. Disordered guest water molecules in (a) are omitted for clarity.

When **6** was exposed to air at room temperature, the color of the crystal turned back to yellow within a few minutes, whereas the crystallinity was still retained. The X-ray analysis of the rehydrated crystal (**2′**) revealed that the coordinated nitrate anions were dissociated from Co atoms and instead water molecules were again coordinated at the apical position. Crystallographic analysis shows that the newly obtained aqua form (**2′**) is almost superimposable on the original structure of **2** (Figure 3c).

The void after removal of water molecules was offset by the distortion of layers rather than by the sliding of frameworks, resulting in a decrease in the cell volume from 4263.9(7) to 4036.0(16) $Å^3$. The framework distortion made the distance between Co atoms shorter by 0.25 Å. The disordering of flexible ethylene glycol chains also offset the void. The mobility of carbon and oxygen atoms in the side chain significantly increased in the absence of guest molecules, as shown by the ORTEP drawing of the square-grid cavity (Figure 4).

The use of $Ni(NO_3)_2 \cdot 6H_2O$ in place of $Co(NO_3)_2 \cdot 6H_2O$ resulted in the same square-grid framework,[11] $\{[Ni(\mathbf{1})_2(H_2O)_2](NO_3)_2 \cdot 1.5H_2O\}_n$ (**3**), which, as expected, contains the same

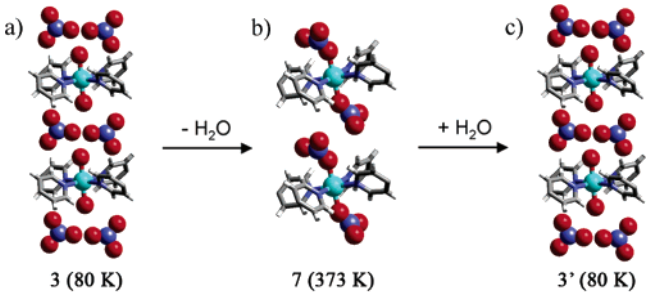

Figure 5. Crystal views around the nickel ion of (a) original crystal **3**, (b) the crystal after heating at 373 K (**7**), and (c) the crystal after exposure of **7** to air (**3′**). Two other disordered nitrate anions are omitted for clarity.

infinite 1D hydrogen bond arrays as that of **2**. The distance between oxygen atoms of hydroxyl groups in **3** is also ca. 2.60 Å, similar to that in **2**. This ligand-exchange process in **3** was also confirmed by crystallographic analysis. Two water molecules are coordinated to the nickel(II) center at the apical positions as well as four pyridyl groups at equatorial positions (Figure 5a). The reversible exchange behavior between aqua and nitrate ligands is similar to that of **2**. The crystallographic analysis at 373 K reveals that the apical water molecules are substituted by two nitrate anions and released out of the crystal to give nitrate in the form of complex $[Ni(\mathbf{1})_2(NO_3)_2]_n$ (**7**) (Figure 5b). Upon exposure of **7** to air at room temperature, it turned back to the initial aqua form (**3′**) (Figure 5c). However, the color change of **3**, depending on the temperature, was not observed clearly during the ligand-exchange process, which is different from that of **2**.[12]

Chromic Behavior of 2. A temperature-dependent color change of the crystal was correlated with the ligand-exchange process in the cobalt metal. The diffuse reflectance UV−vis spectrum of **2** had a main band at about 480 nm (Figure 6a). The removal of water molecules caused the intensity to decrease, and a new band appeared at approxi-

(11) The nickel(II) center is also octahedrally coordinated to four pyridyl groups at the equatorial positions (Ni−N_{Py_1}, 2.102(3) Å; Co−N_{Py_2}, 2.206(3) Å), and two water molecules at the apical positions (Ni−O_{H_2O} 2.080(4) Å). These values are typical of Ni(II)−pyridyl aqua complexes. (a) Turner, D. R.; Hursthouse, M. B.; Light, M. E.; Steed, J. W. *Chem. Commun.* **2004**, 1354. (b) Carlucci, L.; Ciani, G.; Proserpio, D. M.; Rizzato, S. *CrystEngComm* **2003**, 190. (c) Aakeroy, C. B.; Beatty, A. M.; Leinen, D. S. *Angew. Chem., Int. Ed.* **1999**, *38*, 1915.

(12) It is reasonable because a $Ni(II)(py)_4(NO_3)_2$ complex is pearl blue, as are Ni(II)−pyridyl aqua complexes. Soldatov, D. V.; Lipkovshi, Y.; Grachev, E. V. *J. Struct. Chem.* **1995**, *36*, 912.

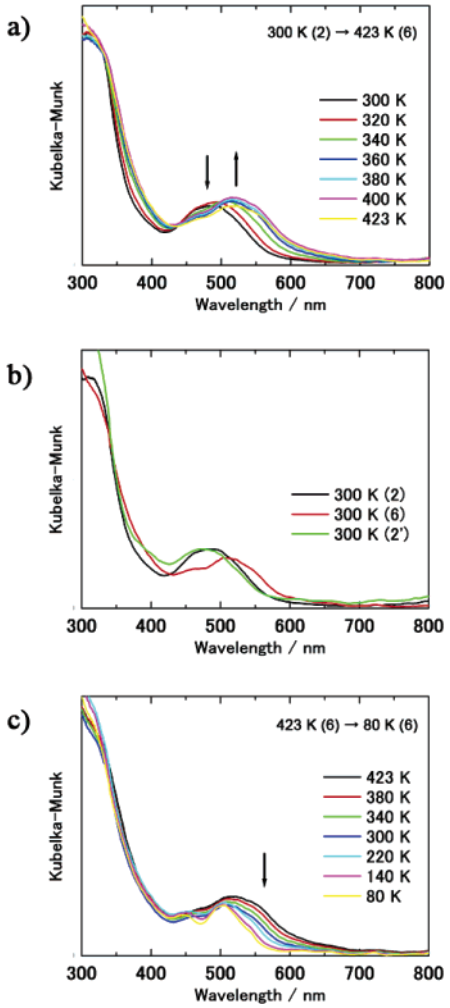

Figure 6. Diffuse reflectance UV−vis spectrum of **2**, **6**, and **2′**. (a) UV−vis spectral change of **2** in the range of 300−423 K, accompanied by the apical-ligand exchange (**2** to **6**). (b) UV−vis spectra of **2**, **2′**, and **6** at 300 K. (c) UV−vis spectral change of **6** in the range of 423−80 K.

mately 522 nm instead. Heating the crystal from 360 to 423 K showed a slight change in the UV−vis spectrum, whereas a significant change was observed at 300−360 K, which corresponds to the dehydration temperature. Cooling **6** down to 300 K resulted in a reflectance spectrum different from that of **2** at the same temperature, and consecutively, after exposing it to air overnight, the spectrum returned to almost the original one of **2** (Figure 6b). The reversible spectral change was accompanied by the apical ligand exchange between aqua and nitrate ligands. This fact indicates that the chromic property of **2** is principally ascribed to the difference of the ligand-field splitting energy of the d-orbitals of cobalt induced by apical-ligand exchange. It is reasonable that the nitrate anion, which has a weaker ligand-field-splitting ability compared with water, decreases the HOMO−LUMO energy gap, followed by a red shift of the absorption bands. The energy-level change also influences the geometrical parameters of the cobalt center: Co−O_{H_2O} 2.095(4) Å to Co−O_{NO_3} 2.129(8) Å; Co−N_{Py_1} from 2.160(3) to 2.144(5) Å; Co−N_{Py_2} from 2.142(3) to 2.129(5) Å. The change of the adsorption band around 550 nm of **6** assignable to d−d transitions was observed depending on the temperature (Figure 6c).[13] The chromic behavior is reversible in the range of 80−423 K under a N_2 atmosphere.

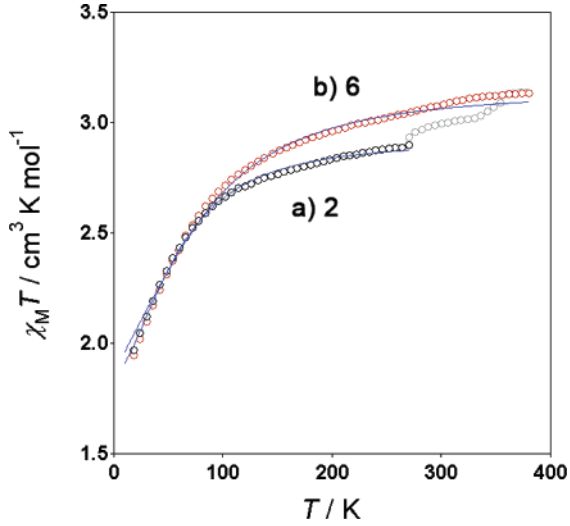

Figure 7. Plots of temperature dependence χ_MT for (a) **2** (green), cooling from 270−15 K, and (b) **6** (red), cooling to 15 K after heating from 270−380 K. The blue line indicates the best fit for experimental data.[17]

Magnetic Property of 2 and 6. The temperature dependence of the magnetic susceptibility for aqua form **2** and nitrate form **6** were measured as shown in Figure 7 ($\chi_M T$ vs T curve), where χ_M is the molar magnetic susceptibility. The $\chi_M T$ values at 270 K were 2.90 cm^3 K mol^{-1} for **2** and 3.05 cm^3 K mol^{-1} for **6**, which are larger than that expected for the spin-only value (1.875 cm^3 K mol^{-1}, Co(II); $S = 3/2$). The $\chi_M T$ values gradually decreased with decreasing temperature. This gradual decrease at low temperature is considered to be a typical manner of zero-field splitting energy (D) due to the octahedral geometry of Co(II). Using the equation that accounts for D on Co(II) (eq 3), the $\chi_M T-T$ plots were fit, where N is Avogadro's number and θ is the magnetic interaction between Co(II) molecules.[14,15] The best fit for the experimental data of **2** leads to $g = 2.50(1)$, $|D| = 68(1)$ cm^{-1}, and $\theta = 0.2(2)$ K. The temperature-dependent magnetic behavior of **6** can be modeled as well, with values of $g = 2.60(1)$, $|D| = 97(3)$ cm^{-1}, and $\theta = 0.1(4)$ K. The reason the $\chi_M T$ values at 270 K for **2** and **6** are larger than the expected value is the contribution of the orbital magnetic moment of Co(II). The obtained D values are consistent with the reported values of typical octahedral Co(II).[16] The small θ values show antiferromagnetic interactions between near-

(13) Cotton, F. A.; Wilkinson, G. *Advanced Inorganic Chemistry*, 5th ed.; John Wiley: New York, 1986; pp 729−732. Although the thermochromism may be explained by d-orbital energy-level changes, single-crystal X-ray analysis shows that the geometry of the cobalt(II) center in the nitrate form **6** changed little with changing temperatures in the range 423−80 K: Co−O_{NO_3} from 2.129(8) to 2.150(3) Å; Co− N_{Py_1} from 2.146(5) to 2.147(3) Å; Co− N_{Py_2} from 2.127(5) to 2.124(3) Å.

(14) Kahn, O. *Molecular Magnetism*; VCH: New York, 1993.

(15) Noveron, J. C.; Lah, M. S.; Del Sesto, R. E.; Ariff, A. M.; Miller, J. S.; Stang, P. *J. Am. Chem. Soc.* **2002**, *124*, 6613.

(16) (a) Herrera, J. M.; Bleuzen, A.; Dromzée, Y.; Julve, M.; Lloret, F.; Verdaguer, M. *Inorg. Chem.* **2003**, *42*, 7052. (b) Tuna, F.; Golhen, S.; Ouahab, L.; Sutter, J. P. *C. R. Chim.* **2003**, *6*, 377.

(17) Aqua form **2** gradually turns to nitrate form **6** by dehydration above room temperature. The fitting was performed below 270 K, because in the range of 270−380 K, two types of 2D coordination networks exist as a mixture of **2** and **6**.

Table 1. Crystal Data for **2**, **6**, **2′**, and **5**

	2	**6** (423 K)	**6** (80 K)	**2′**	**5**
empirical formula	$C_{40}H_{28}N_6O_{20}Co$	$C_{40}H_{28}N_6O_{14}Co$	$C_{40}H_{28}N_6O_{14}Co$	$C_{40}H_{28}N_6O_{20}Co$	$C_{35}H_{24}N_6O_{13}Co$
fw	971.61	875.61	875.61	971.61	795.53
T (K)	80(2)	423(2)	80(2)	80(2)	80(2)
cryst syst	*Pbcn*	*Pbcn*	*Pbcn*	*Pbcn*	*Cc*
space group	orthorhombic	orthorhombic	orthorhombic	orthorhombic	monoclinic
Z	4	4	4	4	4
a (Å)	23.681(2)	23.092(5)	23.025(3)	23.677(3)	
b (Å)	20.617(2)	20.572(5)	20.722(3)	20.576(2)	16.860(2)
c (Å)	8.7636(8)	8.496(2)	8.279(1)	8.7155(9)	15.697(2)
β (deg)	90	90	90	90	15.255(2)
V (Å^3)	4263.7(8)	4036.0(16)	3950.2(10)	4246.0(8)	112.062(2)
D_{calcd} (g cm^{-3})	1.514	1.441	1.472	1.520	3741.5(7)
μ (mm^{-1})	0.493	0.501	0.512	0.495	1.412
R_1 [$I > 2\sigma(I)$]	0.0805	0.1039	0.0785	0.0985	0.0722
wR_2 [$I > 2\sigma(I)$]	0.2361	0.2384	0.1904	0.2592	0.2029

est-neighbor Co(II) molecules. This is explained by the long distance between Co(II) in the crystal, i.e., cobalt(II) molecules are well-separated by ca. 15 Å (intralayer) and ca. 8.6 Å (interlayer).

$$\chi_M = \frac{1}{3}\left[\frac{N\mu_B{}^2 g^2}{4k(T-\theta)}\frac{1+9e^{-2D/kT}}{(1+e^{-2D/kT})}\right] + \frac{2}{3}\left[\frac{N\mu_B{}^2 g^2}{k(T-\theta)}\frac{1+(3kT/4D)(1-e^{-2D/kT})}{1+e^{-2D/kT}}\right] \quad (3)$$

Conclusion

We proposed a new design for constructing a square-grid coordination polymer via the modification of a ligand. In this study, the infinite 1D hydrogen-bond chains composed of ethylene glycol chains contribute to the stabilization of the 2D coordination framework, keeping the environment of substitution-active metal sites. We also succeeded in apical-ligand-exchange reactions on cobalt and nickel ions within a square-grid coordination network in a single-crystal-to-single-crystal fashion. Crystallographic and spectroscopic studies revealed that the temperature-dependent color change of the crystal was attributed to the ligand-exchange process between H_2O and a NO_3 anion on the cobalt metal.

By utilizing the fluid cavity within a rigid grid framework, we have realized the in situ crystallographic observation of the dynamic process that involves drastic structural change around the reaction center. Flexible frameworks that interact with exchangeable guest molecules in a switchable fashion can be promising in developing advanced materials such as molecular sensing devices.

Experimental Section

Materials and Methods. ^{1}H, ^{13}C NMR, and other 2D NMR spectra were recorded on a Bruker DRX-500 (500 MHz) spectrometer. Reagents and solvents were obtained from TCI Co. Ltd., WAKO Pure Chemical Industries Ltd., and Aldrich Chemical Ltd. and were used without further purification. Diffuse UV−vis reflectance spectra were measured on a Jasco V-550 spectrometer equipped with an integrating sphere accessory with a cryostat system (Oxford OptistatDN-V) and were converted from reflection to absorbance by the Kubelka−Munk method. IR spectra were measured on a DIGILAB FTS2000S instrument by the ATR method. Thermogravimetric analyses were carried out on Netzsch STA-409 PG Luxx at a heating rate of 2 K min^{-1} in a dynamic nitrogen atmosphere (gas flow rate of 70 mL min^{-1}). Magnetic measurements on a polycrystalline sample were carried out by a Quantum Design MPMS-XL superconducting quantum interference device (SQUID) magnetometer. Pascal's constants were used to determine the diamagnetic contribution.

Table 2. Crystal Data for **3**, **7**, and **3′**

	3	**6**	**3′**
empirical formula	$C_{40}H_{28}N_6O19Ni$	$C_{40}H_{28}N_6O14Ni$	$C_{40}H_{28}N_6O_{19}Ni$
fw	953.39	867.33	955.39
T (K)	80(2)	373(2)	80(2)
cryst syst	*Pbcn*	*Pbcn*	*Pbcn*
space group	orthorhombic	orthorhombic	orthorhombic
Z	4	4	4
a (Å)	23.481(2)	23.000(5)	23.401(9)
b (Å)	20.527(2)	20.625(4)	20.501(8)
c (Å)	8.8844(8)	8.502(2)	8.723(3)
β (deg)	90	90	90
V (Å^3)	4282.2(7)	4033.2(14)	4185 (3)
D_{calcd} (g cm^{-3})	1.479	1.428	1.517
μ (mm^{-1})	0.540	0.557	0.553
R_1 [$I > 2\sigma(I)$]	0.0701	0.0982	0.1165
wR_2 [$I > 2\sigma(I)$]	0.1966	0.2009	0.2613

Single-Crystal X-ray Crystallography. Single-crystal X-ray diffraction data were collected on a Bruker Smart 1000 CCD diffractometer with a cryostat system equipped with a N_2 generator (Japan Thermal Eng. Co. Ltd.) using graphite-monochromated Mo Kα radiation ($\lambda = 0.71073$ Å) by the ϖ scan mode. The program SAINT was used for integration of the diffraction profiles. Empirical absorption corrections were applied by using the SADABS program. The structures were solved by direct methods (SHELXS97) and refined by full-matrix least-squares calculations on F^2 (SHELXL97) using the SHELXTL program package. Hydrogen atoms were fixed at calculated positions and refined with a riding model. Several restraints were applied to disordered nitrate ions, ethylene glycol groups, and water molecules. The crystal data for **2**, **6**, **2′**, and **5** are summarized in Table 1. The crystal data for **3**, **7**, and **3′** are summarized in Table 2. The crystallographic details are described in the CIF files deposited with the CCDC (No. 250540 (**2**), 250541 (**6**, 423 K), 292923 (**6**, 80 K), 250542 (**2′**), 292857 (**3**), 292859 (**7**), 292858 (**3′**), and 250611 (**5**)). These data can be obtained free of charge via www.ccdc.cam.ac.uk/data_request/cif or by emailing data_request@ccdc.cam.ac.uk.

Preparation of 1. 2,3-Bis(2-hydroxyethoxy)-1,4-diiodo-benzene: A solution of NaOH (4.0 g, 100 mmol) in H_2O (100 mL) was added in portions to a stirred mixture of 1,4-diiodo-2,3-dihydroxybenzene (7.24 g, 20 mmol) and 2-bromoethanol (12.4 g, 100 mmol) in H_2O under N_2. The temperature of the reaction mixture should be below 30 °C. When the addition was completed, the temperature was raised to 90 °C and the mixture was stirred

for 3 h. After cooling the mixture to 40 °C, we added H_2SO_4 (0.3 mL). The resulting mixture was stirred at 25 °C for 4 h; the colorless powder was separated by filtration, dried, and purified by recrystallization from AcOEt to yield 2,3-bis(2-hydroxyethoxy)-1,4-diiodo-benzene as a colorless powder (4.15 g, 46%).

A mixture of 2,3-bis(2-hydroxyethoxy)-1,4-diiodo-benzene (2.12 g, 5 mmol), 4-pyridylboronic acid ester (2.56 g, 12.5 mmol), K_3PO_4 (7.80 g, 37.5 mmol), and $[Pd(PPh_3)_4]$ (300 mg) in dioxane (100 mL) was refluxed under an Ar atmosphere for 2 days (eq 1). After removal of the dioxane, the residue was purified by flash chromatography (1/:20 MeOH:$CHCl_3$) to give **1** as a colorless powder (1.06 g, 60%).

Physical Data of 1. ^{1}H NMR (500 MHz, $CDCl_3$, 300 K): δ 8.68 (d-like, $J = 5.0$ Hz, 4H, PyH_α), 7.56 (d-like, $J = 5.0$ Hz, 4H, PyH_β), 7.27 (s, 2H, Ar*H*), 3.89−3.87 (m, 4H, CH_{2a}), 3.74−3.72 (m, 4H, CH_{2b}), 2.06 (br, 2H, OH). ^{13}C NMR (125 MHz, $CDCl_3$, 300 K): δ 150.3 (*C*q), 149.9 (*C*H$_\alpha$), 145.3(*C*q), 134.2 (*C*q), 126.1 (*C*H$_\gamma$), 123.8 (*C*H$_\beta$), 75.9 (*C*H$_{2a}$), 61.4 (*C*H$_{2b}$).

Synthesis of 2. The single crystals of **2** were prepared by layering a methanol solution of $Co(NO_3)_2{\cdot}6H_2O$ (5.8 mg in 1 mL) onto a toluene/methanol solution of **1** (15.0 mg in 2 mL). After the solution was allowed to stand for 4 days, the crystals were isolated by filtration in 76% yield (14.4 mg). Anal. Calcd for $\{[Co(\mathbf{1})_2(H_2O)_2](NO_3)_2{\cdot}1.5H_2O\}_n$ (**2**): C, 50.53; H, 4.98; N, 8.84. Found: C, 50.34; H, 4.86; N, 8.72. IR (ATR, cm^{-1}): 2956, 2914, 2863, 1668, 1616, 1549, 1416, 1332, 1225, 1217, 1128, 1085, 940, 819.

Synthesis of 3. Single crystals of **3** were prepared by layering a methanol solution of $Ni(NO_3)_2{\cdot}6H_2O$ (5.8 mg in 1 mL) onto a toluene/methanol solution of **1** (15.0 mg in 2 mL). After the solution was allowed to stand for 10 days, the crystals were isolated by filtration in 61% yield (11.6 mg). Anal. Calcd for $\{[Ni(\mathbf{1})_2(H_2O)_2](NO_3)_2{\cdot}1.5H_2O\}_n$ (**3**): C, 50.54; H, 4.98; N, 8.84. Found: C, 50.35; H, 4.89; N, 8.62. IR (ATR, cm^{-1}): 2956, 2917, 2867, 1612, 1550, 1410, 1361, 1223, 1214, 1127, 1081, 938, 816, 729.

Acknowledgment. We thank Prof. K. Ogawa, Dr. J. Harada, and Dr. T. Fujiwara (the University of Tokyo) for measuring diffuse UV-vis reflectance spectra.

Supporting Information Available: Molecular structures of **2**, **6**, **2′**, **3**, **7**, **3′**, and **5**; TG/DSC data for **2** and **5** (PDF); and X-ray crystallographic data for **2**, **6**, **2′**, **3**, **7**, **3′**, and **5** (CIF). This material is available free of charge via the Internet at http://pubs.acs.org.

IC052138U